

Chapter 6

Highly Fluorescent Dye for α -Synuclein Aggregation Studies

6.1 ABSTRACT

A characteristic of Parkinson's disease is the presence of Lewy bodies in surviving neurons of the *substantia nigra* region of the brain. Lewy bodies are insoluble protein deposits comprised mostly of α -synuclein (α -syn). Measurements of fluorescent energy-transfer (FET) kinetics can provide site-specific information about the structure, dynamics, degree of aggregation, and fibrillogenesis mechanisms of α -syn. Dyes with high quantum yields, I-SHark and pH-SHark, were synthesized for use as fluorescent labeling reagents on protein cysteine residues. The labeling protocol between these fluorescent dyes and a cysteine residue was created using commercially available *Saccharomyces cerevisiae* Iso-1 cytochrome *c* (cyt *c*). Successful labeling was confirmed by absorption spectroscopy, mass spectrometry, and peptide mapping of tryptic digestion fragments. To further enhance the overlap integral for future study on α -syn intermolecular aggregation, an acceptor, nitrophenol, was also designed to couple with pH-SHark.

6.2 INTRODUCTION

In PD patients, abnormal protein aggregates with mostly α -syn have been found. Unfortunately, the usual tools used in determining protein structure, such as x-ray crystallography and NMR spectroscopy, provide little insight into the structure of these soluble oligomers.¹ Measurements of FET kinetics can provide site-specific information about the structure, dynamics, degree of aggregation, and fibrillogenesis mechanisms of amyloid forming proteins.² This powerful tool can be employed to obtain a distribution of distances between a fluorescent donor (D) and an energy acceptor (A),³⁻⁷ as the dipole-dipole energy transfer rates are inversely proportional to the sixth power of the fluorescent D-A distance.⁸ Hence, this technique may extend the understanding of the mechanism of many misfolding diseases, including Alzheimer's⁹ and Parkinson's diseases.¹⁰

To successfully extract distance information between a fluorescent donor and an acceptor, Förster distance (R_0) is an important factor to be considered. Förster distance (**Equation 1**) is dependent on the orientation factor of the transition dipoles of donor and acceptor (κ^2), the refractive index of the surrounding medium (n), the donor fluorescent quantum yield (Φ_D), the normalized donor fluorescence spectrum (F_D), the acceptor molar absorption spectrum (ϵ_A), and the wavelength (λ).

$$R_0^6 = 8.785 \times 10^{-5} \frac{\kappa^2}{n^4} \Phi_D \int F_D(\lambda) \epsilon_A(\lambda) \lambda^4 d\lambda \quad (1)$$

Currently, we have been using tryptophan and 3-nitrotyrosine as our fluorescent donor and energy acceptor (D-A), respectively, to characterize the

monomeric structure of α -syn.² However, the Förster distance between tryptophan and 3-nitrotyrosine may be too short to measure the distances for aggregation studies.¹¹ Therefore, there is a need to develop a fluorescent label with a higher quantum yield. The biexponential fluorescence decay of tryptophan¹² also complicates data interpretation. Therefore, this chapter describes the development of FET labels with a single exponential decay.

It is also particularly important that the fluorescent label is small enough to not interfere with the native protein structure, and also allow for the maximal rotational freedom of the attached probes.¹ Other requirements of FET labels for protein folding studies include a site-specific labeling reaction and an easy purification protocol for the labeled protein.

In addition, a new energy acceptor was also developed. An iodine is engineered in the label to undergo S_N2 reaction with the sulfhydryl group in the cysteine. Cyt *c*, a well-studied protein with a native cysteine residue, was successfully labeled with the new dyes to prove that they are promising probes for FET studies.

In studying α -synuclein aggregation, an α -synuclein mutant was used to illustrate that it is feasible to label protein with the new energy acceptor. Furthermore, a double cysteine mutant was expressed to investigate whether it is possible to selectively label α -synuclein at two separate sites, one with a fluorescent donor and one with an energy acceptor. This chapter reports the synthesis and spectroscopic characterization of new fluorescent labels and energy acceptor, along with their model compounds (**Figure 6.1**).

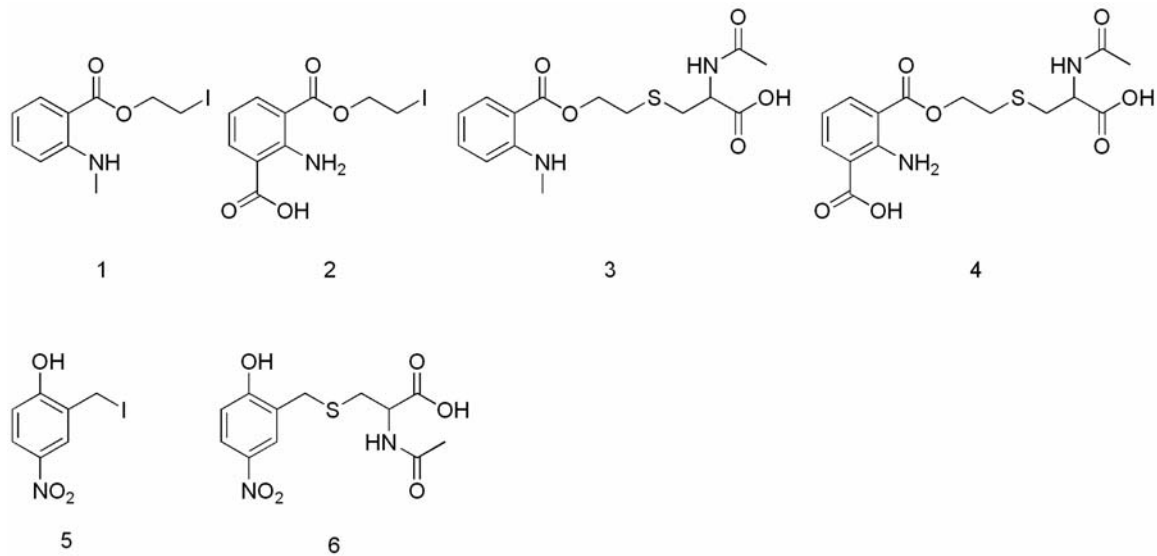


Figure 6.1. Chemical structures of fluorescent labels and their model complexes: I-SHark (1), pH-SHark (2), I-SHark model complex (3), pH-SHark model complex (4), nitrophenol (5), and nitrophenol model complex (6)

6.3 MATERIALS AND METHODS

Materials.

Unless specified otherwise, all the reagents and solvents were purchased from Sigma and VWR, respectively. Thin Layer Chromatography (TLC) was carried out on silica gel plates (Merck 60-F254). The compounds were visualized using UV light (254 nm and 365 nm). Flash chromatography was carried out using silica gel 60 (EMD Chemicals, 40-63 μm). ^1H - and ^{13}C -NMR spectra were collected in CD_3OD with a Varian Inova 300 MHz spectrometer. Mass analyses were conducted by a ThermoQuest LCQ ion trap mass spectrometer by the California Institute of Technology Protein/Peptide Microanalytical Laboratory. All elemental analyses were carried out by Desert Analytics, Inc. (Tucson, AZ).

Synthesis of I-SHark (1) [2-iodoethyl 2-(methylamino)benzoate].

2-(methylamino)-benzoic acid was first recrystallized from CH_2Cl_2 . The recrystallized 2-(methylamino)-benzoic acid (2.55 g, 16.9 mmol), 4-dimethylaminopyridine (DMAP, 320 mg, 2.62 mmol), and 2-iodoethanol (8.56 g, 49.8 mmol) were dissolved in dry CH_2Cl_2 (30 mL). To this mixture, a solution of dicyclohexylcarbodiimide (DCC, 3.80 g, 18.4 mmol) in dry CH_2Cl_2 (10 mL) was added dropwise. The mixture was stirred under Ar at room temperature for 5 h. The solution was filtered through celite, washed with CH_2Cl_2 , dried over Na_2SO_4 , and concentrated under vacuum. The concentrated solution was purified under flash column chromatography (hexanes/ethyl acetate 10:1). The purified green oil was

then acidified with concentrated HCl. The chloride salt was crystallized from methanol/ether. Yield: 1.56 g, 30%. $R_f = 0.62$ (hexanes/ethyl acetate 10:1). $^1\text{H NMR}$ (300 MHz, CD_3OD): δ 8.17 (1H, dd, $J = 8.1, 1.2$ Hz), 7.70 (1H, dt, $J = 8.4, 1.5$ Hz), 7.28-7.34 (2H, m), 4.61 (2H, t, $J = 6.6$ Hz), 3.54 (2H, t, $J = 6.6$ Hz), 3.07 (3H, s). $^{13}\text{C NMR}$ (300 MHz, CD_3OD): -0.8, 35.5, 66.1, 119.9, 121.6, 127.2, 132.2, 135.4, 140.7, 165.5. ESI-MS m/z 306 ($M + 1$). Anal. Calcd. for $\text{C}_{13}\text{ClH}_{13}\text{INO}_2$: C, 35.16; Cl, 10.38; H, 3.84; I, 37.15; N, 4.10; O, 9.37. Found: C, 35.23; H, 3.88; I, 37.61; N, 4.11.

Synthesis of pHI-SHark (2) [2-amino-3-[(2-iodoethoxy)carbonyl]benzoic acid].

DMAP (27 mg, 0.2 mmol) and 2-iodoethanol (781 mg, 4.45 mmol) were added to a stirring solution of 2-aminoisophthalic acid (274 mg, 1.50 mmol) in THF (20 ml). A solution of DCC (340 mg, 1.65 mmol) was then added dropwise. After stirring for 4 h at room temperature, the mixture was dried under vacuum. The residue was redissolved in diethyl ether and extracted with 5% aqueous NaHCO_3 (3×30 mL). The aqueous layers were combined and acidified with 6M HCl to pH 5–6 and then extracted with ethyl acetate (3×30 mL). Further acidification of the aqueous layer to pH < 4 permitted recovery of the starting material, 2-aminoisophthalic acid. The organic phases were combined and dried over MgSO_4 , filtered, and concentrated under reduced pressure to yield a pale yellow solid. The crude product was purified by chromatography (diethyl ether/hexanes 3:1), dissolved again in methanol by adding 6M NH_4OH , and crystallized from methanol/dichloromethane. Yield: 48 mg, 14%. $R_f = 0.56$ (ethyl acetate/hexanes/acetic acid 3:1:0.01). $^1\text{H NMR}$ (300 MHz, CD_3OD): δ 8.05 (1H, dd,

$J = 7.5, 1.8$ Hz), 7.96 (1H, dd, $J = 7.8, 1.8$ Hz), 6.50 (1H, t, $J = 7.8$ Hz), 4.49 (2H, t, $J = 6.6$ Hz), 3.48 (2H, t, $J = 6.6$ Hz). ^{13}C NMR (300 MHz, CD_3OD): -0.2, 64.8, 111.0, 112.1, 113.4, 137.2, 138.1, 149.1, 167.1, 176.9. ESI-MS m/z 334 ($M - 1$). Anal. Calcd. for $\text{C}_{10}\text{H}_9\text{INNaO}_4$: C, 33.64; H, 2.54; I, 35.54; N, 3.92; Na, 6.44; O, 17.92. Found: C, 33.58; H, 2.72; I, 34.97; N, 3.86.

Synthesis of I-SHark Model Compound (3) [2-(acetylamino)-3-[(2-[[2-(methylamino)benzoyl]oxyethyl]thio]propanoic acid].

To a stirring solution of **1** (305 mg, 1.00 mmol) and N-acetyl-cysteine (326 mg, 2.00 mmol) in dry DMF (20 ml), 1,8-Diazabicyclo[5.4.0]undec-7-ene (DBU, 608 mg, 4.00 mmol) in DMF was added dropwise. The mixture was stirred under Ar for 1 h. The solution was reduced to dryness under vacuum and redissolved in 1M HCl. The solution was then extracted with ethyl acetate (3 \times 30 mL). The organic layers were reduced to dryness under vacuum and redissolved in methanol. After adding 10 μl of 30% NH_4OH solution, the product was crystallized from methanol/ether. Yield: 92 mg, 27%. $R_f = 0.46$ (dichloromethane/methanol/acetic acid 4:1:0.1); ^1H NMR (300 MHz, CD_3OD): δ 7.87 (1H, dd, $J = 8.1, 1.8$ Hz), 7.36 (1H, dt, $J = 8.4, 1.8$ Hz), 6.70 (1H, d, $J = 8.4$ Hz), 6.56 (1H, dt, $J = 8.4, 1.2$ Hz), 4.47 (1H, dd, $J = 7.2, 4.2$ Hz), 4.37 (2H, t, $J = 6.6$ Hz), 3.15 (1H, dd, $J = 13.8, 4.5$ Hz), 2.89-2.98 (6H, m), 1.99 (3H, s). ^{13}C NMR (300 MHz, CD_3OD): 21.6, 28.4, 30.7, 34.9, 54.5, 63.1, 109.7, 110.6, 114.2, 118.1, 131.5, 134.6, 152.2, 171.6, 175.8. ESI-MS m/z 363 ($M + \text{Na}$). Anal. Calcd. for $\text{C}_{15}\text{H}_{23}\text{N}_3\text{O}_5\text{S}$: C, 50.41; H, 6.49; N, 11.76; O, 22.38; S, 8.97. Found: C, 49.61; H, 6.24; N, 11.49; S, 8.37.

Synthesis of pHI-SHark Model Compound (4) [3-[(2-[[2-(acetylamino)-2-carboxyethyl]thio]ethoxy)carbonyl]-2-aminobenzoic acid].

To a stirring solution of **2** (108 mg, 0.3 mmol) in dry DMF (6 ml), DBU (182 mg, 1.2 mmol) and N-acetyl-cysteine (98 mg, 0.6 mmol) were added. After stirring for 18 h under Ar at room temperature, the mixture was concentrated under reduced pressure and redissolved in water. The solution was acidified with 37% HCl (100 μ l) and extracted with ethyl acetate (3 \times 30 mL). The organic extracts were washed with water and dried with MgSO₄. The solution was dried under reduced pressure and redissolved in methanol. After adding 30% NH₄OH (20 μ l), the product was crystallized by methanol/ethyl ether. Yield: 32 mg, 32%. R_f = 0.66

(dichloromethane/methanol/acetic acid 4:1:0.1). ¹H NMR (300 MHz, CD₃OD): δ 8.10 (1H, dd, J = 6.6, 1.8 Hz), 8.07 (1H, dd, J = 6.6, 1.8 Hz), 6.57 (1H, t, J = 7.8 Hz), 4.51 (1H, dd, J = 7.8, 4.5 Hz), 4.42 (2H, t, J = 6.6 Hz), 3.16 (1H, dd, J = 13.8, 4.5 Hz), 2.90-2.97 (3H, m), 2.00 (3H, s). ESI-MS m/e 393 (M + Na). Anal. Calcd. for C₁₅H₁₇N₂O₇S: C, 46.51; H, 5.46; N, 10.85; O, 28.91; S, 8.28. Found: C, 45.51; H, 5.40; N, 9.55; S, 8.31.

Synthesis of Nitrophenol (5).

Sodium iodide (660 mg, 4.4 mmol) was dissolved in minimal amount of dry acetone. Under Ar, 2-hydroxy-5-nitrobenzyl bromide (1.031g, 4 mmol) was dissolved in minimal amount of dry acetone in a 100 mL round bottom flask. The sodium iodide solution was then added dropwise into the round bottom flask. The mixture was stirred under Ar for 30 min. Dichloromethane (30 mL) was added to the

reaction mixture. The mixture was then filtered and concentrated to dryness. The dried solid was redissolved in minimal amount of benzene for recrystallization. After recrystallization was completed, the solution was filtered and dried, yielding brown crystals. Yield: 0.935 g (87%) $^1\text{H-NMR}$ ($d_4\text{-CH}_3\text{OH}$), δ : 8.221 (d, 1H, $J = 3.0$ Hz), 8.029 (dd, 1H, $J = 8.8$ Hz, 3.0 Hz), 6.872 (d, 1H, $J = 9.0$ Hz), 4.528 (m, 2H).

Synthesis of Nitrophenol Model Complex (6).

Nitrophenol (861 mg, 3.08 mmol) and N-acetyl-L-cysteine (1 g, 6.16 mmol) were dissolved in minimal amount of anhydrous DMF. A solution of DBU (1.88 g, 0.0123 mmol) in anhydrous DMF was added dropwise into the stirring solution of starting material under Ar. The reaction was allowed to proceed for 2 hr. The DMF was then concentrated under reduced pressure to yield a brown oil. 5 mL of ethyl acetate was added and the solution was then acidified with concentrated HCl until the brown oil was dissolved. The solution was extracted with water (2×30 mL). The aqueous layer was extracted with ethyl acetate (3×30 mL). The combined organic extracts were dried with MgSO_4 . The dried solution was concentrated to 2 mL under reduced pressure and a white precipitate was observed. NH_3OH was added to redissolve the white precipitate and a yellow oil was yielded. The oil was dried and ammonia was removed under reduced pressure. Methanol (5 mL) was added to redissolve the oil and ethyl acetate was added to recrystallize the product. $^1\text{H-NMR}$ ($d_4\text{-CH}_3\text{OH}$), δ : 8.221 (d, 1H, $J = 3.0$ Hz), 8.029 (dd, 1H, $J = 8.8$ Hz, 3.0 Hz), 6.872 (d, 1H, $J = 9.0$ Hz), 4.528 (m, 2H). ESI-MS m/e 293 ($M + \text{Na}$).

Purification of Cyt c.

Commerically available cyt *c* was dissolved in 20 mM NaP_i (pH 7.0) buffer. The 100 μM cyt *c* solution was treated with 1 mM Na₂S₂O₄ and 1 mM DTT. Protein was then purified by ion-exchange chromatography using a Mono S column on a Fast Protein Liquid Chromatography (FPLC) system (Pharmacia). The column was equilibrated with 20 mM NaP_i buffer (pH 7.0) and the protein was eluted using a stepwise salt gradient (0–1 M NaCl), with both buffers containing 1 mM dithiothreitol (DTT). Pure fractions were then combined and concentrated to 50–100 μM. Purity of protein was confirmed using absorption and electrospray mass spectrometry.

Purification of α-Synuclein.

A single cysteine mutant, V40C, was expressed to develop the labeling protocol for nitrophenol on α-synuclein. For the double labeling studies, a double cysteine mutant, V26C/E57C, was selected. The purification protocol for α-synuclein from other chapters, with the addition of 1 mM DTT, was adopted to purify the protein. The purity of the mutant was proved by UV-Vis, SDS-PAGE and mass spectrometry.

Fluorescent Dye Labeling Procedures.

Purified cyt *c* (50–100 μM in NaP_i, pH 7.0) was exchanged into 20 mM NaP_i (pH 7.6) buffer. It was then denatured with 4 M guanidinium chloride (GuHCl) and reduced by the same concentration of Tris(2-carboxy-ethyl)phosphine hydrochloride

(TCEP). The reaction mixture was deoxygenated by repeated evacuation/Ar-fill cycles on a Schlenk line for 30 min. pH-I-SHark (twentyfold molar excess) was dissolved in the same buffer (1 ml) and added dropwise to the stirring solution of the protein. The reaction was performed in the dark to minimize deleterious photochemical side reactions. The procedures for I-SHark labelling were slightly modified. Twentyfold molar excess of I-SHark was dissolved in 10% DMSO. The concentrated dye solution was added in two portions (at beginning of the reaction and after 12 h) in order to enhance the solubility of the dye.

The labelling reaction was stirred at room temperature for 40 h. Prior to purification, the solution was centrifuged at $10000 \times g$ for 30 min to remove the insoluble dye. The protein was then oxidized with a tenfold excess of $K_3[Fe(CN)_6]$ for 30 min. The reaction mixture was desalted on a gel filtration column (HiPrep Desalting 26/10) using FPLC run in 20 mM NaP_i (pH 7.0). Dye-labeled protein was separated by ion-exchange chromatography (Mono S column) using a shallow stepwise salt gradient (0–1 M NaCl) in 20 mM NaP_i (pH 7.0). All the dye-labeled proteins were stored in the dark at 4 °C.

The labeling reaction was proven successful by UV-Vis spectroscopy, ESI-MS and SDS-PAGE. Trypsin digestion was also performed with the labeled protein by the California Institute of Technology Protein/Peptide Microanalytical Laboratory. The peptide fragments were then analyzed by MALDI-MS. The results demonstrate that the dye was correctly labeled onto the desired cysteine residue.

Energy Acceptor Labeling Procedures.

Concentrated α -synuclein mutant V40C ($\sim 100 \mu\text{M}$) was stirred in the dark with a twentyfold molar excess of TCEP for 30 min. A twentyfold excess of nitrophenol was then added to the stirring protein. The reaction was stopped by applying the reaction mixture to the gel filtration column (HiPrep 26/10) on FPLC. The desalted protein solution was then purified by ion-exchange chromatography (Mono Q). The purity of the labelled protein was confirmed by UV-Vis and ESI-MS.

Double Cysteine Labeling Procedures.

In the dark, a twentyfold molar excess TCEP was stirred with concentrated α -synuclein mutant V26C/E57C ($\sim 100 \mu\text{M}$) for 30 min. A tenfold molar excess of 1,5-I-AEDANS was then added to the stirring protein. The reaction was stopped by applying the reaction mixture to the gel filtration column (HiPrep 26/10) on FPLC. The desalted protein solution was then purified by ion-exchange chromatography (Mono Q). The singly labelled protein was characterized by UV-Vis and ESI-MS. It was then concentrated and labelled with nitrophenol using the same protocol as above.

Steady-State Spectroscopy.

Spectroscopic measurements for folded protein were recorded at room temperature with samples dissolved in phosphate buffer (20 mM NaP_i , pH 7.4), while 6 M guanidinium chloride (GuHCl) was added for the unfolded samples. Samples were deoxygenated by repeated evacuation/Ar-fill cycles during a period of 30 min

and sealed in fused-silica fluorescence cuvettes (1 cm × 1 cm). Absorption and luminescence spectra were measured on a Hewlett-Packard 8452 diode array spectrophotometer and a Spex Fluorolog2 spectrofluorimeter, respectively.

Evaluation of the Förster distance.

The value of overlap integral (J , **Equation 2**) for the donor-acceptor pairs (I-SHark/heme and pHl-SHark/heme) was determined using the absorption spectrum for cyt c and normalized emission spectra of compounds **3** and **4**. The solution refractive index (n) was taken to be 1.34,¹³ while the orientation factor (κ^2) was averaged to be 2/3 for the random dynamic orientation of the donor and acceptor.

$$J = \int F_D(\lambda)\epsilon_A(\lambda)\lambda^4 d\lambda \quad (2)$$

Time-Resolved Fluorescence Spectroscopy.

Samples for time-resolved fluorescence spectroscopy measurements were prepared as described above. Samples were excited by a 355 nm polarized pulse (35° from vertical) generated from a mode-locked Nd:YAG laser regenerative amplifier. Emission above 420 nm was selected by cutoff filters. Decay kinetics were measured with a picosecond streak camera (Hamamatsu C5680) in single photon counting mode. All experiments were controlled by a temperature-controlled cuvette holder at 25 °C. Control experiments were conducted using the model complexes **3** and **4**.

Data Analysis.

The measured fluorescence decay kinetics by non negative linear least-squares (NNLS) protocol, and were thoroughly described in Chapter 1.¹⁴

6.4 RESULTS AND DISCUSSION

Dye Synthesis.

The new labels and their corresponding model compounds (cysteinic conjugates) were successfully synthesized by one-step reactions. The products were easily purified by either flash column chromatography or recrystallization.

When designing the structure of new FET labels, minimal perturbation of the native protein structure and high rotational freedom of the dyes were considered. Therefore, I-Shark, pHI-SHark and nitrophenol were designed to cause minimal steric hindrance. Iodoacetamide is frequently used as the reactive site for cysteine labeling. However, iodine was chosen instead in designing these labels to provide higher conformational freedom. The fluorophore conformational freedom was further enhanced by the ethylenic chain linking the cysteine and fluorophore.

Protein Labeling.

The functionalization of cyt *c* involves a linker between the fluorescent probe and Cys102 of the protein. However, the thiol of Cys102 is not solvent-exposed enough to react with the labels. Therefore, the protein was unfolded by GuHCl to encourage protein derivatization. TCEP was also added to avoid the oxidation of

sulphur groups. The reaction was carried out at a pH = 7.6 to where the thiol group was partially deprotonated, while the amine side chain of lysine, which is a main reactive agonist of cysteine, was almost fully protonated. The duration of protein labeling was optimized at 40 h, as protein denaturation and the oxidation of thiolic groups reduce labeling yields at longer reaction times.

Labeling α -synuclein has proven to be much easier as the protein is unstructured. Only 3 h of reaction was needed to yield labeled protein. After successfully labeling α -synuclein at one site, double cysteine labeling was attempted to investigate the possibility of tagging a fluorescent donor and an energy acceptor onto the same protein molecule. The dually labeled protein could be used to extract long-range intramolecular distances. The two cysteine labeling dyes chosen for this experiment were dansyl (Dns) and nitrophenol (NP). Dns and NP were chosen as robust cysteine labeling protocols have been developed previously.

Figure 6.2 shows the FPLC traces during the protein purification process after dansyl labeling was completed. Proteins from both peaks were submitted for UV-Vis and mass spectrometry analysis. The first peak was identified as the singly dansyl-labeled protein, while both cysteine sites were labeled by dansyl in the second peak. Protein fractions from the first peak were subjected to nitrophenol labeling.

Figure 6.3 shows the FPLC traces after nitrophenol labeling. Two peaks were again identified. Mass spectrometry and UV-Vis have confirmed that proteins from both peaks were labeled with dansyl and nitrophenol. It will require mass spectrometry on the tryptic digest product of those fractions to see which one contains V26C-Dns/E57C-NP and V26C-NP/E57C-Dns.

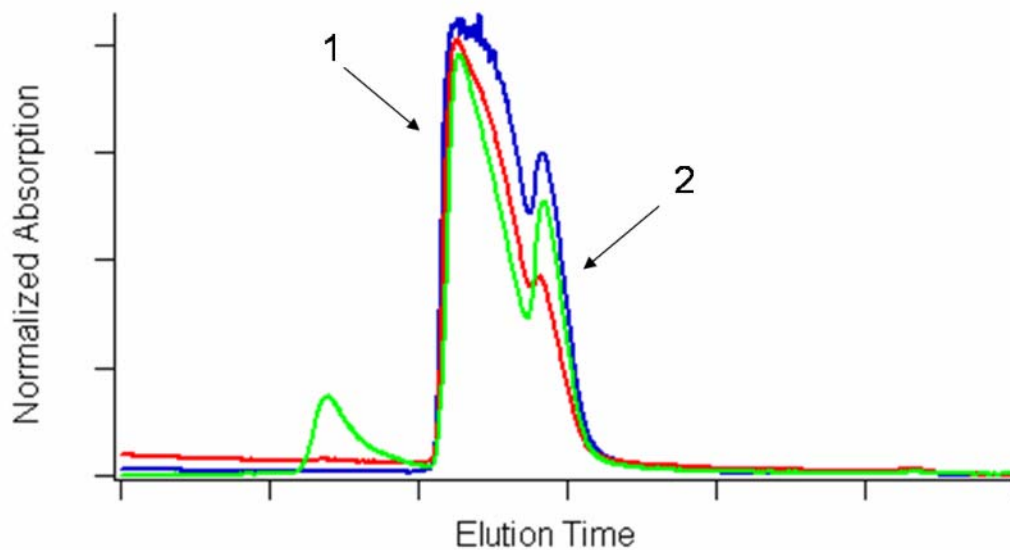


Figure 6.2. The FPLC traces during the protein purification process after dansyl labeling was completed. Peak (1) was identified as the singly dansyl-labeled protein, while both cysteine sites were labeled by dansyl in the second peak. Absorptions were monitored at 215 nm (blue), 280 nm (red), and 355 nm (green).

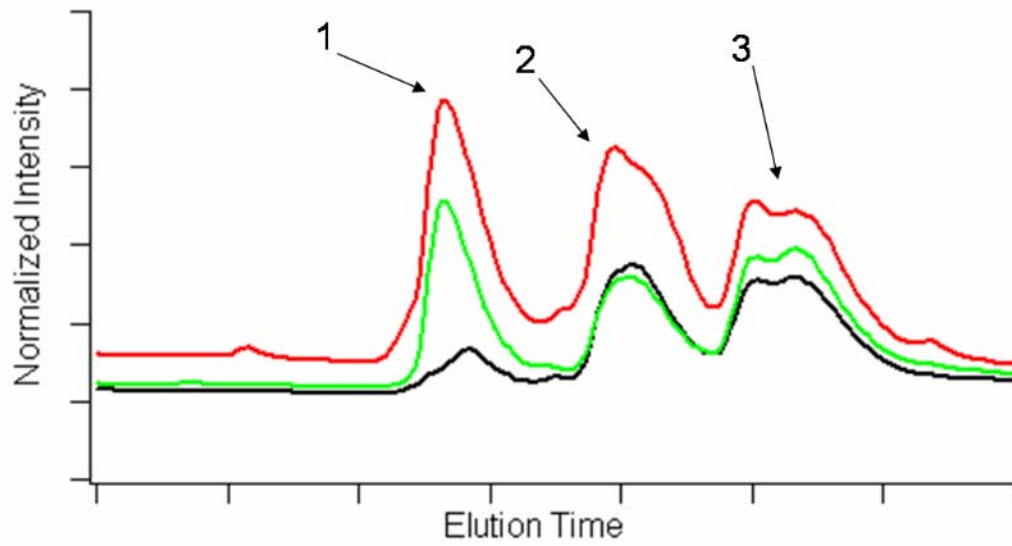


Figure 6.3. The FPLC traces after nitrophenol labeling, with absorption detected at 280 nm (red), 355 nm (green), and 400 nm (black). Peak (1) corresponds to protein that was not labeled with nitrophenol. Peak (2) and Peak (3) highlighted could be V26C-Dns/E57C-NP and V26C-NP/E57C-Dns.

Spectroscopic Characterization.

Previously, the fluorescent quantum yields of the labels, calculated overlap integral, and Förster distances between I-SHark/phI-SHark and cyt *c* heme group have been determined (**Table 6.1**). The overlap between the absorption of cyt *c* and phI-SHark is better than that of cyt *c* and I-SHark (**Figure 6.4**). It is also demonstrated that the fluorescence of phI-SHark has a higher quantum yield and longer Förster distance with cyt *c* than I-SHark. Another distinct disadvantage of I-SHark is its poor water solubility. DMSO was added to enhance dye solubility in the labeling reaction. However, the amount of DMSO added (10% v/v) was limited to avoid protein precipitation. On the contrary, the second carboxylic acid group makes phI-SHark more soluble than I-SHark in the aqueous labelling environment. Since phI-SHark has been shown to be a better label, our following discussion will be focused on the spectroscopic characterization of phI-SHark.

The phI-SHark-labeled cyt *c* was characterized spectroscopically in its native and denatured conformation to illustrate the ability of the label to provide distance information. When the protein is folded, the distance between Cys102 to the iron heme center is 13.9 Å. Therefore, when the protein is folded, the fluorescence emitted by the label should be quenched by the heme group.

On the other hand, when the protein is unfolded, the distance between the heme group and fluorophore should be too large for the quenching to be effective. In fact, steady-state fluorescence spectra show a significantly reduced emission for the folded protein compared to the unfolded protein (**Figure 6.5**). FET kinetics (**Figure 6.6**) also show a much faster decay for the folded protein ($6 \times 10^{-9} \text{ s}^{-1}$, 80%), when

	Quantum Yield	Förster Distance (Å)	Overlap Integral ($M^{-1} cm^{-1} nm^4$)
I-Shark	0.32	50	8.7×10^{14}
phI-SHark	0.48	60	8.1×10^{15}

Table 6.1. Fluorescent quantum yields of I-SHark and phI-SHark, calculated overlap integral and Förster distances between I-SHark/phI-SHark and heme group

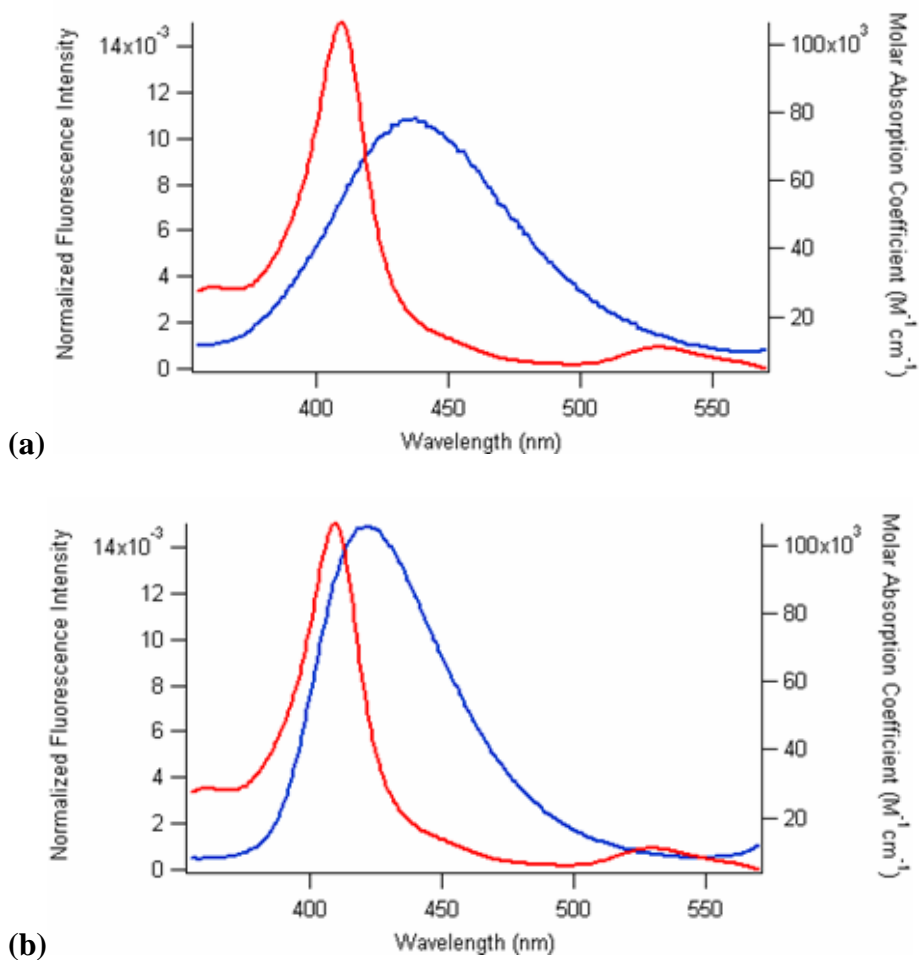


Figure 6.4. Molar absorption spectra of cyt c (red line), and fluorescence spectra (blue line) of (a) I-SHark and (b) pH-SHark

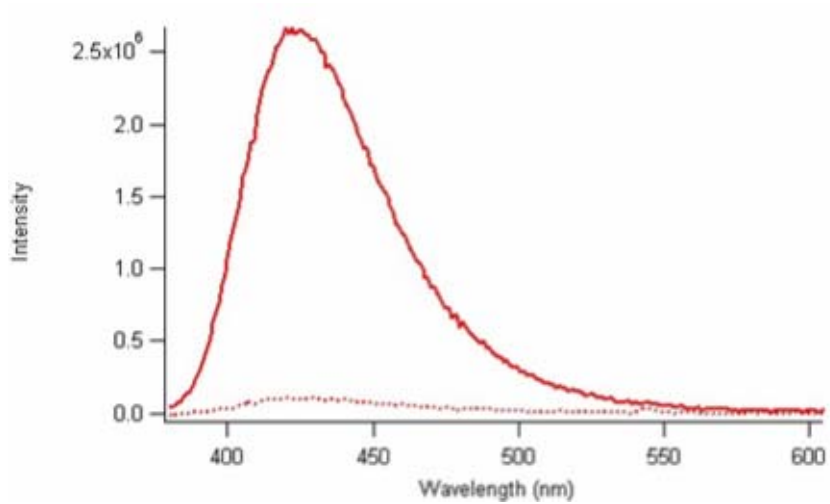


Figure 6.5. Steady-state fluorescence spectra for 5 μ M pHl-SHark labeled cyt *c* in 20 mM NaPi (dotted line) and 6 M GuHCl (solid line), pH 7.4 at 25 $^{\circ}$ C

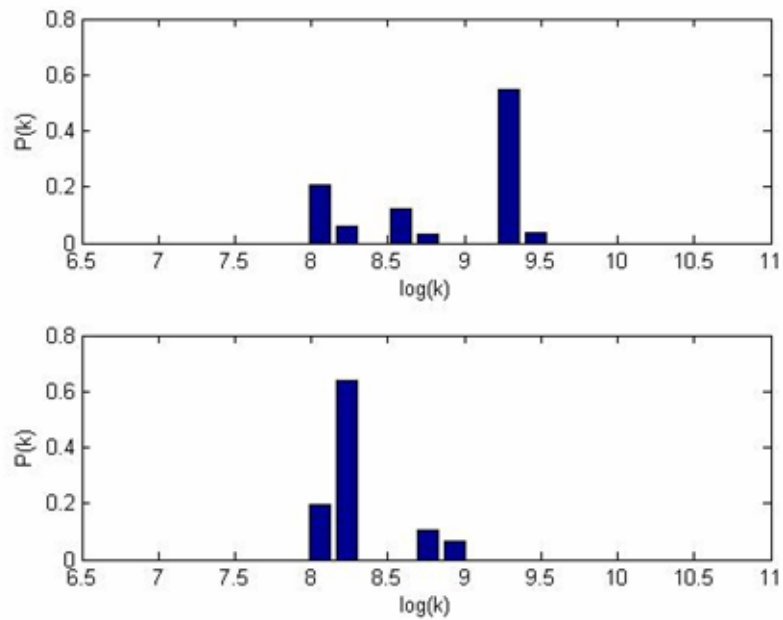


Figure 6.6. Distribution of fluorescence decay rates, $P(k)$, for 5 μM pHl-SHark labeled cyt c in 20 mM NaP_i (top panel) and 6 M GuHCl (bottom panel) at pH 7.4 and 25°C, from NNLS analyses of the FET kinetics

compared to the unfolded protein ($8 \times 10^{-9} \text{ s}^{-1}$, 30%, $5 \times 10^{-10} \text{ s}^{-1}$, 60%).

Control experiments using the pH-SHark model complex in NaP_i buffer and 6 M GuHCl were conducted. Comparable steady-state fluorescence emissions (**Figure 6.7**) and time-resolved lifetimes (**Figure 6.8**) show that pH-SHark behaves similarly in buffer ($8 \times 10^{-9} \text{ s}^{-1}$, 90%) and high concentration of GuHCl ($7 \times 10^{-9} \text{ s}^{-1}$, 90%). It can also be noted that the unquenched emission of pH-SHark is singly exponential.

Finally, pH-SHark and nitrophenol were developed as the fluorescent donor and energy acceptor for intermolecular FET studies during aggregation events.

Figure 6.9 shows the overlap between the fluorescence of pH-SHark (blue line) and absorption of nitrophenol (red line). The Förster distance was calculated to be 42 Å for this D-A pair, allowing us to measure distances between 13 and 65 Å.

In summary, two highly fluorescent dyes, I-SHark and pH-SHark, and an energy acceptor, nitrophenol, were synthesized and characterized. Spectroscopic characterization of pH-SHark-labeled cyt *c* shows that pH-SHark fulfills the requirements needed for an excellent label for FET studies. The overlap integral between pH-SHark and nitrophenol also allows for a large Förster distance which allows study of α -synuclein aggregation. Minimal steric hindrance, high rotational freedom, single exponential fluorescent lifetime, high quantum yield, ease of synthesis, and high solubility in water make pH-SHark-nitrophenol attractive as a fluorescent donor-energy acceptor pair to provide long-range distance information during protein folding events.

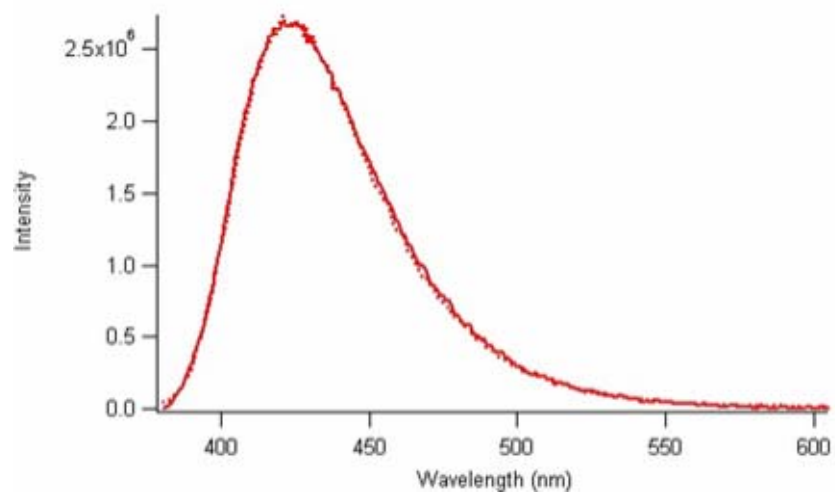


Figure 6.7. Steady-state fluorescence spectra for 5 μ M pHI-SHark model complex (4) in 20 mM NaP_i (dotted line) and 6 M GuHCl (solid line), pH 7.4 at 25 °C.

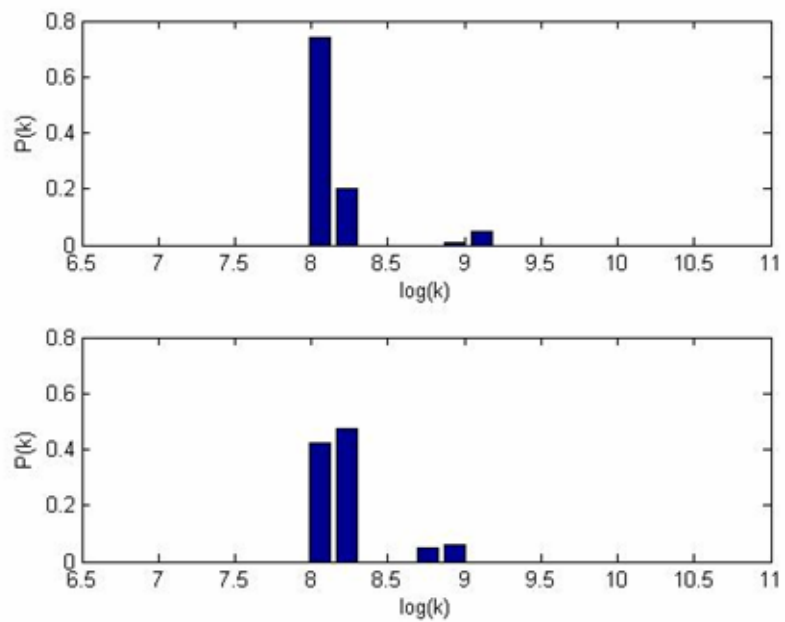


Figure 6.8. Distribution of fluorescence decay rates, $P(k)$, for 5 μM pHl-SHark model complex (**4**) in 20 mM NaP_i (top panel) and 6 M GuHCl (bottom panel) at pH 7.4 and 25 $^\circ\text{C}$, from NNLS analyses of the FET kinetics

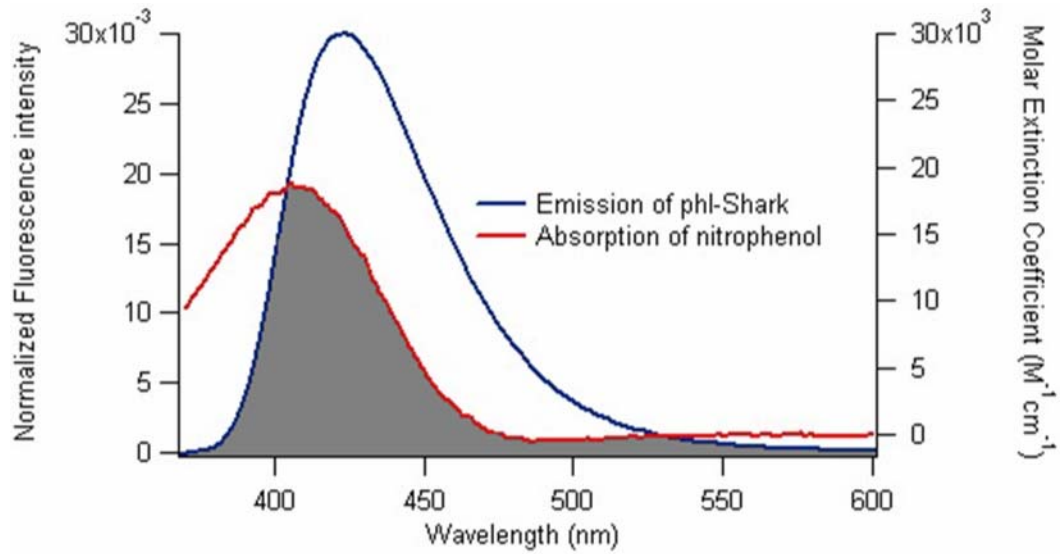


Figure 6.9. Molar absorption spectra of nitrophenol (red line), and fluorescence spectra (blue line) of pHl-SHark

6.5 ACKNOWLEDGEMENT

Synthetic and labeling protocols for I-SHark and pH-SHark were developed by Dr. Seth B. Harkins, Dr. Francesco Bellia, and Dr. Jennifer C. Lee. This work was performed in collaboration with Mr. Dustin D. Hawker.

6.6 REFERENCES

- (1) Duus, J. O. *J. Phys. Chem. B* **1998**, *102*, 6413–6418.
- (2) Lee, J. C.; Langen, R.; Hummel, P. A.; Gray, H. B.; Winkler, J. R. *Proc. Natl. Acad. Sci. U. S. A.* **2004**, *101*, 16466–16471.
- (3) Lyubovitsky, J. G.; Gray, H. B.; Winkler, J. R. *J. Am. Chem. Soc.* **2002**, *124*, 14840–14841.
- (4) Lee, J. C.; Engman, K. C.; Tezcan, F. A.; Gray, H. B.; Winkler, J. R. *Proc. Natl. Acad. Sci. U. S. A.* **2002**, *99*, 14778–14782.
- (5) Wu, P. G.; Brand, L. *Anal. Biochem.* **1994**, *218*, 1–13.
- (6) Navon, A.; Ittah, V.; Landsman, P.; Scheraga, H. A.; Haas, E. *Biochemistry* **2001**, *40*, 105–118.
- (7) Pletneva, E. V.; Gray, H. B.; Winkler, J. R. *J. Am. Chem. Soc.* **2005**, *127*, 15370–15371.
- (8) Forster, T. *Ann. Phys.-Berlin* **1948**, *2*, 55–75.
- (9) Phu, M. J.; Hawbecker, S. K.; Narayanaswami, V. *J. Neurosci. Res.* **2005**, *80*, 877–886.
- (10) Winkler, G. R.; Harkins, S. B.; Lee, J. C.; Gray, H. B. *J. Phys. Chem. B* **2006**, *110*, 7058–7061.
- (11) Callis, P. R. *J. Phys. Chem. B* **2004**, *108*, 4248–4259.
- (12) Szabo, A. G.; Rayner, D. M. *J. Am. Chem. Soc.* **1980**, *102*, 554–563.
- (13) Thormahlen, I. *J. Phys. Chem. Ref. Data* **1985**, *14*, 933–946.
- (14) Lee, J. C.; Lai, B. T.; Kozak, J. J.; Gray, H. B.; Winkler, J. R. *J. Phys. Chem. B* **2007**, *111*, 2107–2112.